Al-Nahrain University, College of Engineering Journal (NUCEJ) Vol.19 No.2, 2016 pp.228 - 245

Finite Element Modeling and Theoretical Analysis of SFRSCC Composite Beams Strengthened by Bottom Tensioned Steel Plates

Laith Khalid Al-Hadithy
Department of Civil Engineering
Al-Nahrain University/ Iraq
E-mail:lthadithy@yahoo.com

Maryam Abdul Jabbar Hassan
Department of Civil Engineering
Al-Nahrain University/ Iraq
E-mail:maryem_aj@yahoo.com

Abstract

This research concern finite element modelling and theoretical analysis for evaluating the effect of steel fibers on the behaviour of composite beams of tensioned steel-concrete interfaces with shear connectors. Based on available experimental tests of seven composite beams consisting of rectangular reinforced concrete prisms (125*200*1900)mm strengthened by bottom steel plates interconnected by shear connectors, of diverse contents of steel fiber volume fraction (0.0%, 0.2%, 0.5% and 0.8%), shear connectors distributions and plates thicknesses and lengths. Each beam was loaded up-to failure under the influence of two concentrated loads to monitor its failure mode, record the load and deflection values at its mid-span and also register values of the final relative end slip. The proposed nonlinear ANSYS (version 14) model for the seven test beams includes modelling of concrete, steel rebars, steel plates and the steel plate-concrete interface, where the high agreement of the ANSYS-model predictions with the experimental evidence is a definite witness to the reliability of the numerical model. The maximum differences in ultimate loads and mid-span deflection values for all beams are 8.1%% and 7.8%, respectively.

KeyWords: Finite Element Modeling, Steel fiber reinforced self-compacting concrete, steel plate, shear connector, ultimate load and fracture pattern.

Abbreviations:

SCC: Self-**C**ompacting **C**oncrete
SFRSCC: Steel **F**iber **R**einforced **S**elf-**C**ompacting **C**oncrete

Introduction

Composite beams of square or rectangular reinforced concrete sections strengthened by bottom steel plates firmly interconnected by headed-stud shear connectors offer a number of advantages in both design and construction and have been used in a diversity of applications. Their use in buildings and bridges of long spans has been increased in the recent years for the benefit of increased load-carrying capacity. There are benefit of increased load-carrying capacity. There are many advantages of the steel plate-concrete composite (SPCC) structures. To increase live-load capacity, e.g. of a bridge subject to increased vehicle loads or a building the use of which is to change from residential to commercial, there is no concrete cover outside the steel plate, so the weight of the structure can be reduced, especially for slabs; and there is no crack exposed at the bottom of the structures. The steel plate can be used as formwork during construction and can resist stresses in any direction, which is more effective than reinforcement bars. The structure is applicable blast resistant shelters. The SPCC can also be used in strengthening and rehabilitating existing structures **(Nie Jianguo et al., 2001)[1]** such as concrete bridge by strengthening the decks and girders.

Scope and Significance

This work is devoted to study the behavior of rectangular-section composite beams consisting of self-compacting reinforced concrete prisms (with four values for steel fibers volume fraction (V_f): 0.0%, 0.2%, 0.5% and 0.8%) strengthened by bottom steel plates connectors. Accordingly, this program has been directed to observe the flexural and shear behavior of such beams differing from each other by one or other of three quantitative and dimensional parameters of their components. Based on the experimental results of the loading tests of the seven composite beams, Finite Element Analysis (ANSYS 14.0) software package is used to analyze and determine the load-deflection relations and the crack pattern

.

Details of the Analyzed Composite Beams

Table 1 and Fig. 1: show the details of the analyzed composite beams

Beam Mark	Thickness of bottom steel plate (mm)	Spacing between shear connectors (mm)	Length of steel plate (mm)	Steel Fiber content (% by Vol.)
B1	3	75	1900	0
B2	3	75	1900	0.2
B3	3	75	1900	0.5
B4	3	150	1900	0.5
B5	4.75	75	1900	0.5
B6	4.75	75	1140	0.5
B7	3	75	1900	0.8

Note: B1, B2, B3 and B7 for steel fiber content effect, B3 and B4 for connector spacing effect, B3 and B5 for plate thickness effect, and B5 and B6 for plate length effect

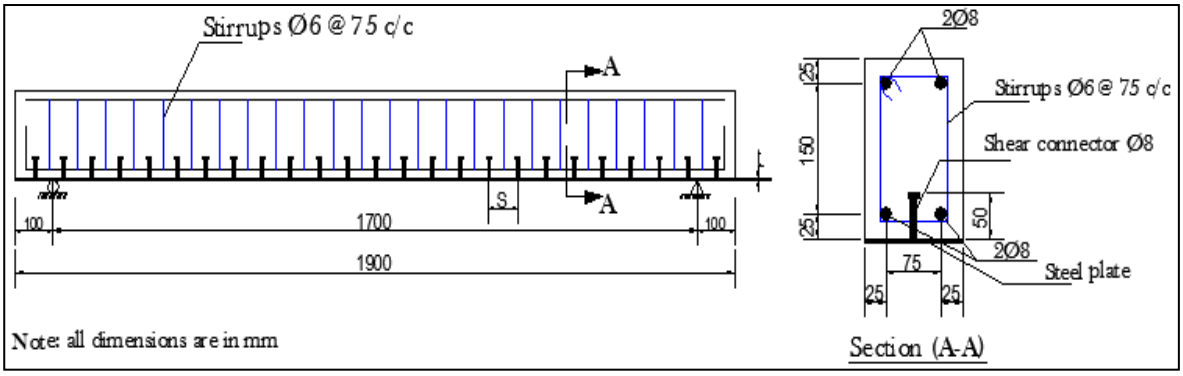

Figure 1: Details of a typical studied beam

Simplified Theoretical Evaluation of the Partial Interaction From Experimental Evidence

To experimentally investigate degrees of the partial interaction at the tensioned steel-concrete interfaces of the seven tested beams, their ultimate flexural strengths have been calculated theoretically (assuming perfect bond at the interfaces specified above) then compared with ultimate load values obtained experimentally.

The ultimate flexural strength values have been calculated by means of the simplified plastic method using the following assumptions:

- The steel plate and the abutting concrete are supposed to be fully integrated.
- The steel plate and the bottom reinforcement are transformed to concrete.
- The stress distribution in the compression concrete zone is assumed to form a rectangular block with disregard of the concrete tensile stresses.
- The steel of the plate and that of the reinforcing bars are assumed not to harden.

A computer program written in *Visual Basic 6.0* language was built to simplify and speed up the calculations

Figure 2 shows the results of the analysis of test beam **B1** calculated by the program. The results of beams **B1** to **B7** are given in Table 2, which illustrates the high degree of interaction for the tested beams where full connection is achieved by the headed studs. It can be also noticed from the table there is great convergence between the experimental and the calculation results where a very high level of convergence as high as **97.74%** has been attained in average (for beams with complete length of bottom steel plate and typical spacings of shear connectors).

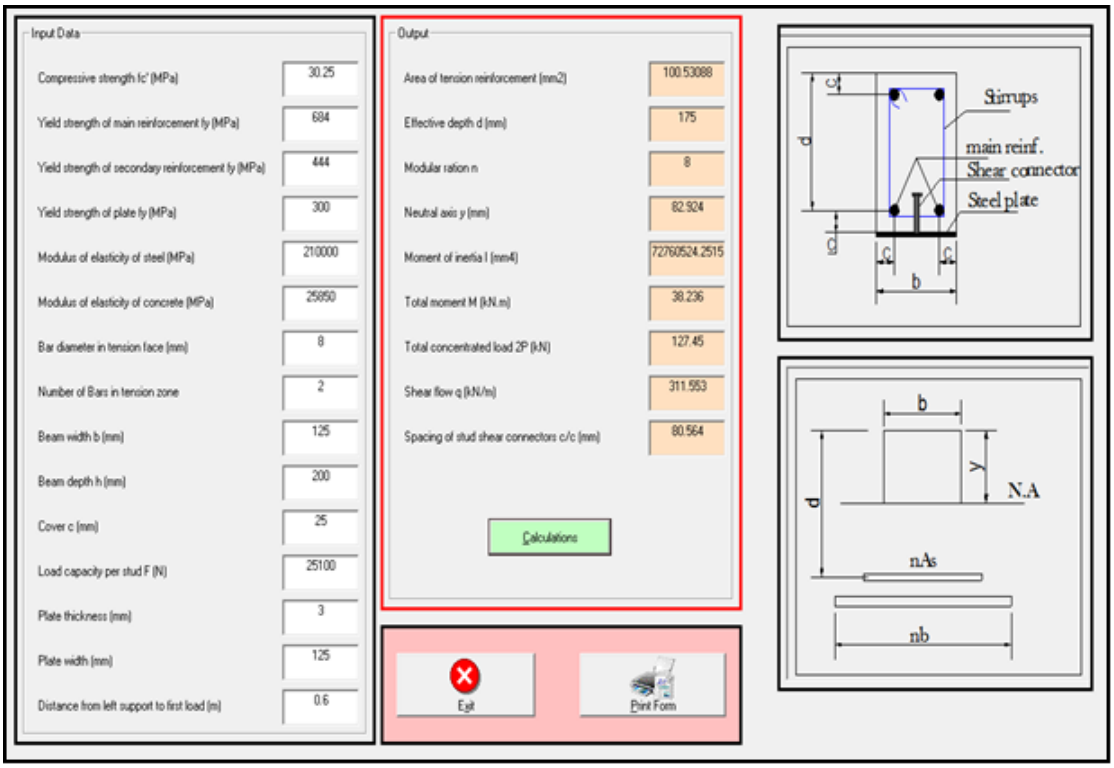

Figure 2: Calculations for beam B1 by Visual Basic 6.0 program

Table 2: Experimental and theoretical ultimate loads

Beam No.		B1	B2	B3	B4	B5	B6	B7
Ultimate Load (kN)	Exp.[1]	120.4	126	134.76	98.77	154.12	67.07	138.08
	Theo.[2]	127.45	129.48	132.55*		154.47**		139.77
Level of coincidence [3]		94.47%	97.31%	101.66%	74.52%	99.77%	43.42%	98.8%

1 Experimental phase of the present study.
2 Theoretical phase of ACI plastic design method **(Nilson, A. H. al et., 2010)[2]** and calculated by Visual Basic 6.0 program
3 Level of coincidence = Ult. P) $_{Exp.}$ / Ult. P) $_{Theo.}$. It gives a close indication to the degree of partial interaction.
* B4 is the same as B3 but with double spacing of shear connectors
** B6 is the same as B5 but with shorter length of steel plate by 40%

Finite Element Model

Software and Element Types

In the present work, the tested beams have been modelled by the finite elements method using ANSYS package (version 14) to investigate the accuracy of this method compared with the experimental results. In ANSYS package, models can be created either by using the command prompt line method which is sometimes called ANSY Parametric Design Language (APDL), or by the Graphic User Interface (GUI).

For the present model, the GUI has been utilized to create the model. Characters of the finite elements types used in modeling each of the seven tested beams by ANSYS program are summarized in Table 3. Each element type in the present model has been used to represent a specified constituent of each of the seven tested beams. **(ANSYS Manual, 2009)[3]**

Table 3: Description of the used element

Beam components		Used element from ANSYS library	Element characteristics
Concrete		SOLID65	8-node Brick Element (3 translational DOF per node)
Steel reinforcing bars (long. top, long. bott., diagonal shear reinforcement and headed studs outside interface)		LINK8	2-node Discrete Element (3 translational DOF per node)
Bottom steel plate		SHELL63	4-node shell Element (3 translational DOF and 3 rotational DOF per node)
Bearing steel plate of loading		SOLID45	8-node Brick Element (3 translational DOF per node)
Interface*	Shear friction and contact	TARGE170 & CONTA174	Nonlinear surface-to-surface interface element
	Dowel Action (shear connectors inside interface)	COMBIN39	2-node zero length nonlinear spring element with one translational DOF per node

* Interface at contact surface between bottom concrete and the steel plate

Material Properties

I) Input Data of Concrete Modelling

Since the elapsing decade it has been well known that the use of small and slender discrete and well-dispersed steel fibers improves the strength; deformability and cracking control of concrete. Hence, fibrous concrete can be used to enhance the behavior of concrete members reinforced with conventional steel reinforcing bars **(Madana et al., 2007)[4]**.

The adopted approach to represent steel fibers in reinforced concrete in the present study is based on the enhancements of the mechanical properties of concrete **(Lihua et al. 2008)[5]**.

Input data for the concrete properties in **ANSYS** computer program are introduced as follows **(Kachlakev et al, 2001)[6]**:

a) Ultimate uniaxial compressive strength (f_c').

b) Modulus of elasticity (E_c).

c) Splitting strength of concrete (f_t).

d) Poisson's ratio (υ).

e) Compressive uniaxial stress-strain relationship for concrete.

f) Shear transfer coefficient for opened and closed cracks (β_o and β_c respectively).

Ultimate uniaxial compressive strength (f_c') and the modulus of elasticity of concrete (E_c) were determined in the laboratory.

The tensile strength of concrete can be estimated using either the modulus of rupture test, split cylinder test or direct tension test. In this study, the tensile stress is calculated from the modulus of rapture test.

Poisson`s ratio of concrete (υ) is the ratio between the transverse and the longitudinal strain when concrete is under longitudinal (axial) stress and it depends somewhat on strength, composition and other factors. At stress lower than about $0.7f_c'$, Poisson's ratio of concrete falls within the limit of 0.15 to 0.2 **(ASTM C1240-03)[7]**. In the present study, it is taken as 0.2.

The compression stress-strain relation for concrete in the present finite element model has been based on the simplified multi-linear isotropic stress-strain model by using the following equations (**Wolanski, 2004)[8]:**

$$f_c = \frac{\varepsilon E_c}{1+\left(\frac{\varepsilon}{\varepsilon_o}\right)^2} \quad \ldots(1)$$

$$\varepsilon_o = \frac{2f_c'}{E_c} \quad \ldots(2)$$

$$f_c = \varepsilon E_c \quad \ldots(3)$$

where:

f_c = Stress at any strain.

ε =Strain at stress f_c .

$\varepsilon_\circ$ = Strain at ultimate compressive strength f_C' .

This simplified model for concrete in compression requires definition of the first point of the curve by the user which has to satisfy Hooke's Law:

$$E = \frac{\sigma}{\varepsilon} \quad \ldots(4)$$

Figure 3 illustrates the stress-strain curve used in the recent research which has proved to be suitable for convergence of the nonlinear solution algorithm.

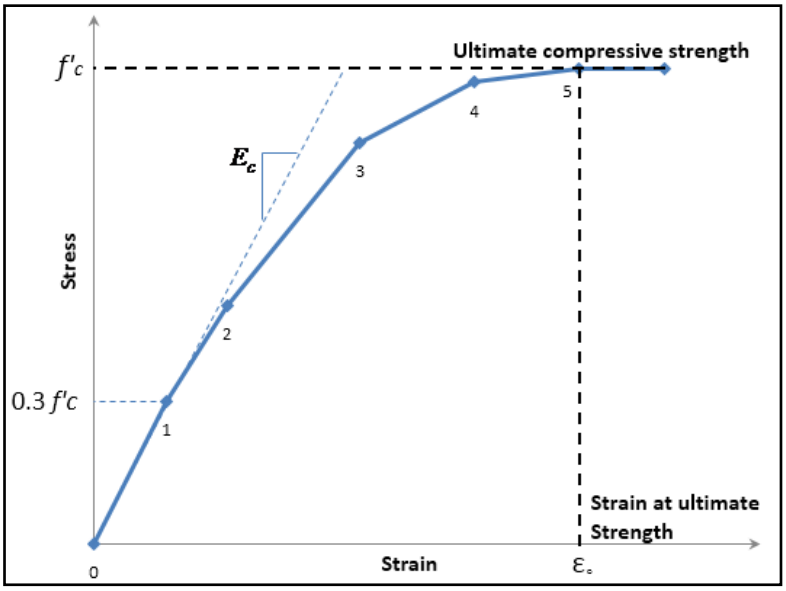

Figure 3: The simplified multi-linear stress-strain curve for uniaxial compression of concrete **(Amer M. Ibrahim 2009)[9]**

The shear transfer coefficient β represents conditions of the crack face. The value of β is limited between 0.0 and 1.0, where 0.0 denote smooth crack representing the complete loss of shear transfer and 1.0 representing a rough crack (no loss of shear transfer) **[3]**. The value of β in this study is influence by the aggregate interlock and the presence of steel fiber in the concrete **(Agwan, 1996)[10]**.

In the present work, the default value of shear transfer coefficient for opened and closed cracks are equal to 0.2 and 0.7 respectively for the non-fibrous concrete **(AL-Taee, 2012)[11]**, while for fibrous concrete the values are 0.3 and 0.8 respectively **[10]**.

The uniaxial crushing stress in the present work has been represented by the uniaxial compressive strength ($f`_c$). As recommended by previous researchers **[6]** the crushing capability of the concrete element has been turned off by entering the crushing stress as -1. Convergence problems have been executed repeating till the crushing capability has been turned off.

ii) Modelling of Steel

The mechanical properties of steel are much simpler to be represented when compared with concrete. The specification of a single stress-strain relation is sufficient to define the material properties needed in the analysis of reinforced concrete.

The strain-stress behavior in tension and compression are similar.

To avoid possible probable numerical complications, the alternative bilinear stress-strain relationship indicated in Fig. 4 may be used in the computer programing.

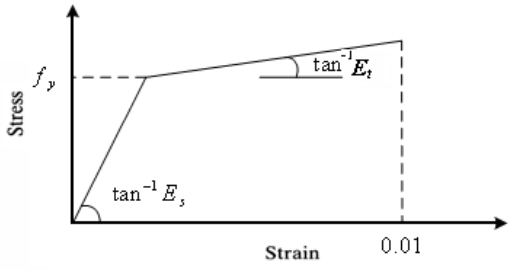

Figure 4: Alternative bilinear stress-strain relationship

In the present work, the strain hardening modulus (E_t) is assumed to be (0.03 E_s). Prevent any suspected iteratively divergent results.

The tensile yield stress and elastic modulus for *steel plate*, *steel bars* and *shear connectors* was calculated from standards tests, while the poisson's ratio was taken 0.3 according to **EC4(1994)[12]**.

iii) Interface Modelling

The term "interface" refers to the region between steel and concrete surface or the precast concrete and cast-in-place concrete surface. These regions are present in any composite beam such as concrete-concrete or concrete-steel and make the finite elements more complex.

An interface is modeled by a medium of no physical thickness called "**contact-pair**" element, which represents two surfaces that are in state of physical contact but may slide relative to each other **[8]**. When deform structural members under external loads, large horizontal forces (shears) are developed that act on the planes of weakness surfaces (interface). Shear forces may be transferred by means of friction between surfaces and by the dowel action of the shear connectors. Two combinations of interface models are used in the present work which is previously explained.

The mechanical behavior of the ***first interface model*** (**CONTA174** & **TARGE170**) is used to simulate the contact surfaces in the basic ***Coulomb friction model*** which is defined the relation between the contact normal pressure (**P**) with the shear stress (**τ**) in the directions normal and tangential to the interface, as shown in Fig. 5.

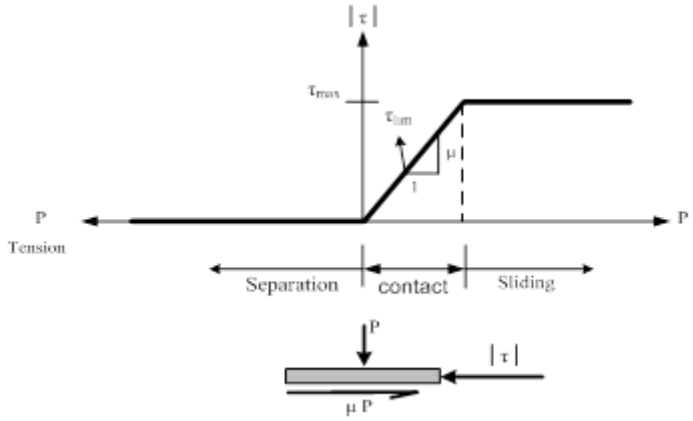

Figure 5: Details of stresses and constitutive relations of the contact surface

In the present work, a coefficient of friction with (μ=0.7) is used between steel plate and concrete. **(ACI 318M-08) [13]**

The ***second interface model*** is used to simulate the normal and dowel stiffness of shear connectors. The normal forces transmitted by the axial forces in the shear connectors are represented in the **ANSYS** model by the link element **LINK8**, while, the shear forces that are resisted by the shear connectors are represented by the nonlinear spring element **COMBIN39**.

When the shear connectors are normal to the plane of interface, dowel action (shearing and flexure of the connectors) will contribute to the overall shear stiffness throughout the contact area. The load-slip values for the headed-stud shear connectors used in the present study are determined experimentally by a standard push out prototype containing the steel shear connectors embedded in self-compacting concrete. The parameters used in the real constants and the material properties, and their numerical values for the tested beams (B1 to B7) are shown in Tables 4 to 7.

Table 4: Parameters identifications and numerical values for element types of the present **ANSYS** model for beam **B1**

Element	Parameter	Definition					Value	
Solid65	f_c'	Ultimate compressive strength(MPa)					30.25	
	f_t	Ultimate tensile strength(MPa)					3.85	
	β_o	Shear transfer parameters					0.2	
	β_c						0.7	
	E_c	Young's modulus of elasticity(MPa)					25000	
	υ	Poisson's ratio					0.2	
	definition of strain-stress relationship for concrete (*SOLID 65*)							
	Stress(MPa)	0	9.1	21.35	27.83	30.05	30.25	30.25
	Strain	0	0.00045	0.001	0.0016	0.00216	0.00242	0.003
Shell63	Parameter	Definition					Value	
	t	Thickness (mm)					3	
	F_y	Yield strength(MPa)					300	
	E_s	Modulus of elasticity(MPa)					193600	
	E_t	Steel hardening(MPa)					5808	
	υ	Poisson's ratio					0.3	
Link8	Parameter	Definition					Value	
	A_b	Cross sectional area (mm^2)					Steel reinforcing main bar Ø8	51.5
							Steel reinforcing stirrups Ø6	32.65
							Shear connector Ø8	50.24
	F_y	Yield tensile stress (MPa)					Steel reinforcing main bar Ø8	684
							Steel reinforcing stirrups Ø6	444
							Shear connector Ø8	350
	E_s & E_t	Modulus of elasticity & strain hardening modulus (MPa)	E_s				Steel reinforcing main bar Ø8	210000
			E_s				Steel reinforcing stirrups Ø6	210000
			E_t				Steel hardening (Ø8,Ø6)	6300
			E_s				Shear connector Ø8	207500
			E_t				Steel hardening Ø8	6225
	υ	Poisson's ratio					Steel reinforcing bars	0.3
							Shear connector	0.3
COMBIN 39	Load-slip relationship for nonlinear spring element (COMBINE39)							
	Load (N)	0	9980	15500	19970	22940	24560	25100	25100
	Slip (mm)	0	1.1	1.91	2.64	3.28	3.91	4.61	5.34
TARGE170 & CONTA174	Parameter	Definition					Value	
	μ	Coefficient of friction					0.7	
Solid45 (for all tested beams)	Modulus of elasticity (MPa)(assumed)						200000	
	Poisson's ratio						0.3	

Table 5: Parameters identifications and numerical values of element types of the present **ANSYS** model for beam **B2**

Element	Parameter	Definition					Value	
Solid65	f_c'	Ultimate compressive strength(MPa)					32.25	
	f_t	Ultimate tensile strength(MPa)					4.39	
	β_o	Shear transfer parameters					0.3	
	β_c						0.8	
	E_c	Young's modulus of elasticity(MPa)					26700	
	υ	Poisson's ratio					0.2	
	definition of strain-stress relationship for concrete (*SOLID 65*)							
	Stress(MPa)	0	9.7	22.75	29.57	31.86	32.25	32.25
	Strain	0	0.00045	0.001	0.0016	0.00216	0.0024	0.003
Shell63	Parameter	Definition					Value	
	t	Thickness (mm)					3	
	F_y	Yield strength(MPa)					300	
	E_s	Modulus of elasticity(MPa)					193600	
	E_t	Steel hardening(MPa)					5808	
	υ	Poisson's ratio					0.3	
Link8	Parameter	Definition					Value	
	A_b	Cross sectional area (mm^2)					Steel reinforcing main bar Ø8	51.5
							Steel reinforcing stirrups Ø6	32.65
							Shear connector Ø8	50.24
	F_y	Yield tensile stress (MPa)					Steel reinforcing main bar Ø8	684
							Steel reinforcing stirrups Ø6	444
							Shear connector Ø8	350
	E_s & E_t	Modulus of elasticity & strain hardening modulus (MPa)	E_s				Steel reinforcing main bar Ø8	210000
			E_s				Steel reinforcing stirrups Ø6	210000
			E_t				Steel hardening (Ø8,Ø6)	6300
			E_s				Shear connector Ø8	207500
			E_t				Steel hardening Ø8	6225
	υ	Poisson's ratio[2]					Steel reinforcing bars	0.3
							Shear connector	0.3
COMBIN 39	Load-slip relationship for nonlinear spring element (COMBINE39)							
	Load (N)	0	9980	15500	19970	22940	24560	25100	25100
	Slip (mm)	0	1.1	1.91	2.64	3.28	3.91	4.61	5.34
TARGE170 & CONTA174	Parameter	Definition					Value	
	μ	Coefficient of friction					0.7	
Solid45 (for all tested beams)	Modulus of elasticity (MPa)(assumed)						200000	
	Poisson's ratio						0.3	

Table 6: Parameters identifications and numerical values of element types of the present **ANSYS** model for beam **B3, B4 – B5, B6**

Element	Parameter	Definition					Value	
Solid65	f_c'	Ultimate compressive strength(MPa)					33.89	
	f_t	Ultimate tensile strength(MPa)					5.29	
	β_o	Shear transfer parameters					0.3	
	β_c						0.8	
	E_c	Young's modulus of elasticity(MPa)					28415	
	υ	Poisson's ratio					0.2	
	definition of strain-stress relationship for concrete (*SOLID 65*)							
	Stress(MPa)	0	10.2	23.85	28.02	31.47	33.89	33.89
	Strain	0	0.00046	0.001	0.0016	0.0022	0.0024	0.003
Shell63	Parameter	Definition					Value	
	t	Thickness (mm)					3 – 4.75	
	F_y	Yield strength(MPa)					300 - 260	
	E_s	Modulus of elasticity(MPa)					193600 - 190800	
	E_t	Steel hardening(MPa)					5808 - 5724	
	υ	Poisson's ratio					0.3	
Link8	Parameter	Definition					Value	
	A_b	Cross sectional area (mm^2)					Steel reinforcing main bar Ø8	51.5
							Steel reinforcing stirrups Ø6	32.65
							Shear connector Ø8	50.24
	F_y	Yield tensile stress (MPa)					Steel reinforcing main bar Ø8	684
							Steel reinforcing stirrups Ø6	444
							Shear connector Ø8	350
	E_s & E_t	Modulus of elasticity & strain hardening modulus (MPa)		E_s			Steel reinforcing main bar Ø8	210000
				E_s			Steel reinforcing stirrups Ø6	210000
				E_t			Steel hardening (Ø8,Ø6)	6300
				E_s			Shear connector Ø8	207500
				E_t			Steel hardening Ø8	6225
	υ	Poisson's ratio					Steel reinforcing bars	0.3
							Shear connector	0.3
COMBIN 39	Load-slip relationship for nonlinear spring element (COMBINE39)							
	Load (N)	0	9980	15500	19970	22940	24560	25100	25100
	Slip (mm)	0	1.1	1.91	2.64	3.28	3.91	4.61	5.34
TARGE170 & CONTA174	Parameter	Definition					Value	
	μ	Coefficient of friction					0.7	
Solid45 (for all tested beams)	Modulus of elasticity (MPa)(assumed)						200000	
	Poisson's ratio						0.3	

Note: B3, B4, B5 and B6 have the same hardening properties (f_c', f_t , E_c), but they are different in the distribution of the shear connectors, thickness and length of the bottom steel plates as indicate in ***Table 1***.

Table 7: Parameters identifications and numerical values of element types of the present **ANSYS** model for beam **B7**

Element	Parameter	Definition					Value	
Solid65	f_c'	Ultimate compressive strength(MPa)					37.75	
	f_t	Ultimate tensile strength(MPa)					7.94	
	β_o	Shear transfer parameters					0.3	
	β_c						0.8	
	E_c	Young's modulus of elasticity(MPa)					30277	
	υ	Poisson's ratio					0.2	
	definition of strain-stress relationship for concrete (*SOLID 65*)							
	Stress(MPa)	0	11.33	27.13	32.56	35.37	37.75	37.75
	Strain	0	0.00052	0.00107	0.0018	0.0023	0.0025	0.003
Shell63	Parameter	Definition					Value	
	t	Thickness (mm)					3	
	F_y	Yield strength(MPa)					300	
	E_s	Modulus of elasticity(MPa)					193600	
	E_t	Steel hardening(MPa)					5808	
	υ	Poisson's ratio					0.3	
Link8	Parameter	Definition					Value	
	A_b	Cross sectional area (mm^2)					Steel reinforcing main bar Ø8	51.5
							Steel reinforcing stirrups Ø6	32.65
							Shear connector Ø8	50.24
	F_y	Yield tensile stress (MPa)					Steel reinforcing main bar Ø8	684
							Steel reinforcing stirrups Ø6	444
							Shear connector Ø8	350
	E_s & E_t	Modulus of elasticity & strain hardening modulus (MPa)	E_s				Steel reinforcing main bar Ø8	210000
			E_s				Steel reinforcing stirrups Ø6	210000
			E_t				Steel hardening (Ø8,Ø6)	6300
			E_s				Shear connector Ø8	207500
			E_t				Steel hardening Ø8	6225
	υ	Poisson's ratio[2]					Steel reinforcing bars	0.3
							Shear connector	0.3
COMBIN 39	Load-slip relationship for nonlinear spring element (COMBINE39)							
	Load (N)	0	9980	15500	19970	22940	24560	25100	25100
	Slip (mm)	0	1.1	1.91	2.64	3.28	3.91	4.61	5.34
TARGE170 & CONTA174	Parameter	Definition					Value	
	μ	Coefficient of friction					0.7	
Solid45 (for all tested beams)	Modulus of elasticity (MPa)(assumed)						200000	
	Poisson's ratio						0.3	

Modeling and Meshing of the Concrete Media, the Bottom Steel Plates and the Bearing Plates

The initial step of modeling includes formation of blocks of the concrete volume, bearing steel plate volumes and the steel plate. Volumes of the concrete and bearing steel plate are formed by specifying keypoints of one side edge of the concrete block and the bearing steel plate, then creating lines between these keypoints to establish the areas and creating volumes by extruding these areas.

Modeling of the bottom steel plate is initiated by introducing keypoints with respect to the origin of coordinates which coincide with external edges of the beam, then formation of the area is bounded by creating lines between those keypoints to create the area of the bottom steel plate.

After creating the concrete media volume, bearing plates volumes and the bottom steel plate area, the finite element model requires their meshing.

After identifying the volumes and the areas, a finite element analysis needs meshing of all the constitutive media in the modeled beam dividing into a number of small elements (rectangular shell elements of 12.5 mm side dimensions). Rectangular meshed are widely preferable for good consequences. Hence rectangular meshing is implemented in the present model.

Figure 6 for beam **B1** shows modeling and meshing of the concrete prism, the bottom interconnected steel plate and bearing the steel plates, with the same fashion for the six remaining beams.

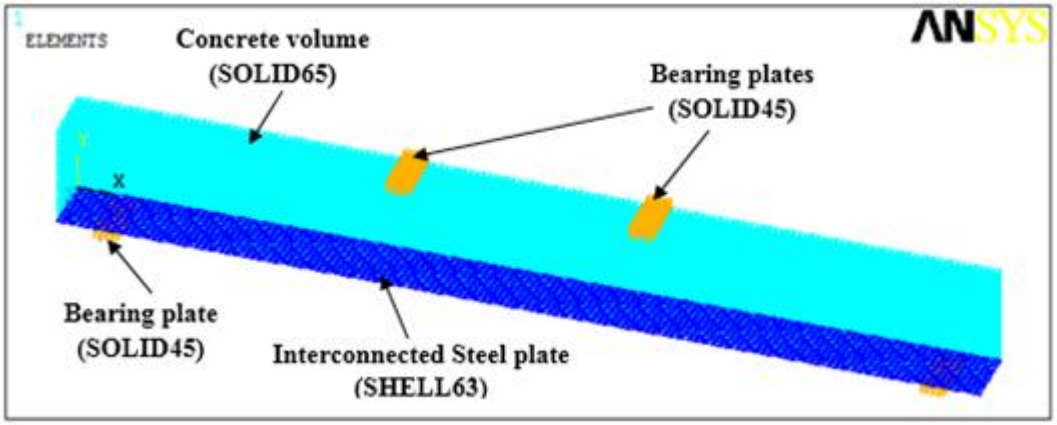

Figure 6: Modeling and meshing of the concrete media, the bottom steel plate, and the bearing steel plates for beam **B1**

Modeling of Steel Reinforcing Bars

For all alignments of the steel reinforcing bars, the discrete element (***LINK8***) has been used as shown in Fig. 7 for beam **B1**. In spite of meshing of volumes for concrete and while volumetric and areal meshings are used for the concrete media and the steel plate, respectively, no meshing for (***LINK8***) elements representing the reinforcing steel bars is needed because individual elements are introduced in the model through the nodes created by volumetric meshing of the concrete media

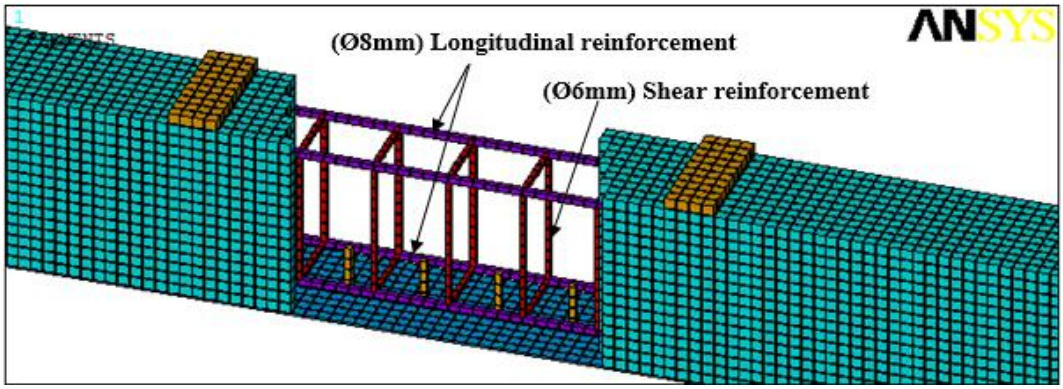

Figure 7: ANSYS modeling of the steel reinforcing bars for beam **B1**

Interface Modeling

Contact-pair (surface-to-surface) elements ***TARGE170*** and ***CONTA174*** have been used for modeling the interface area (contact planes) between the concrete medium and the bottom interconnected steel plate. No mesh is needed there because individual elements have been introduced in the modeling through the boundary surfaces of the meshed concrete media for **CONTA174**, and the bottom interconnected steel plate areas for **TARGE170**. In addition, spring element ***COMBIN39*** has been used to resist the slip, as well as, a discrete element ***LINK8*** (modeling the shear connector) to prevent the uplift separation. Those elements have been used to model the partial interaction, as shown in Fig. 8 for beam **B1**.Meshing of ***COMBIN39*** is usually considered as a special case similar to ***LINK8*** so that ***COMBIN39*** has been created through nodes between concrete volume ***SOLID65*** and steel plate area ***SHELL63*** at interface region, these nodes correspond to the nodes for ***TARGE170*** and ***CONTA174***.

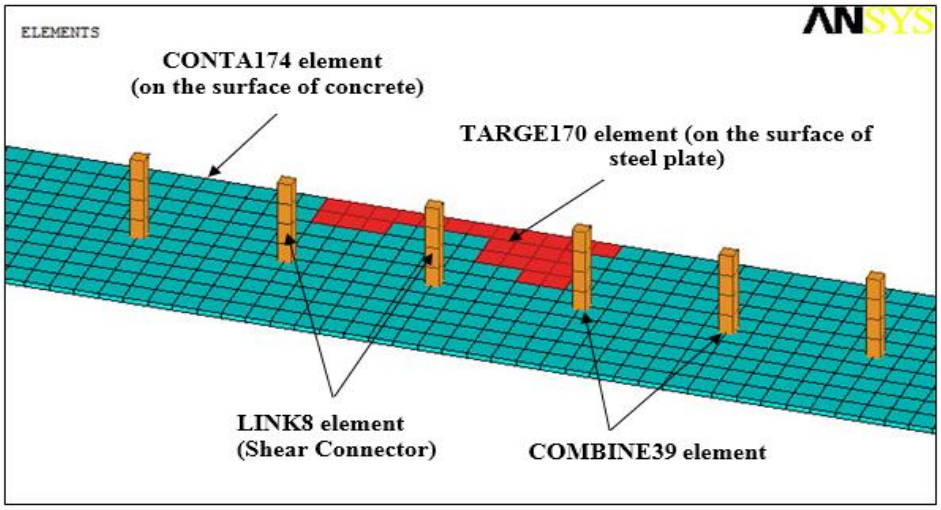

Figure 8: Interface modeling by ANSYS for beam **B1**

Loads and Boundary Conditions

i) Simple supports

The simple support at the left side of the beam has been modeled as a hinge by constraining a single line of bearing plate nodes along the width of the beam soffit in the x- and y-directions (i.e Ux =Uy=0), while the other support has been modeled as a roller by constraining the y-direction (Uy=0), as shown in Fig. 9.

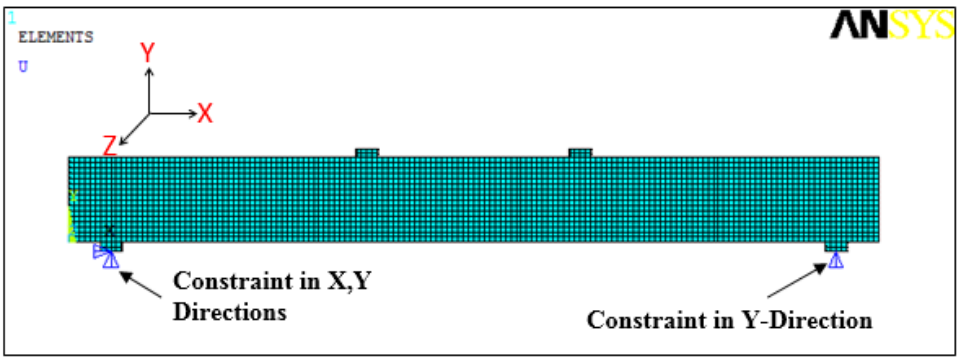

Figure 9: Boundary conditions for simple end supports for beam **B1**

ii) External loads

The external loads has been distributed on the single line of bearing plate nodes across the width of the top surface of the beam as shown in Fig. 10.

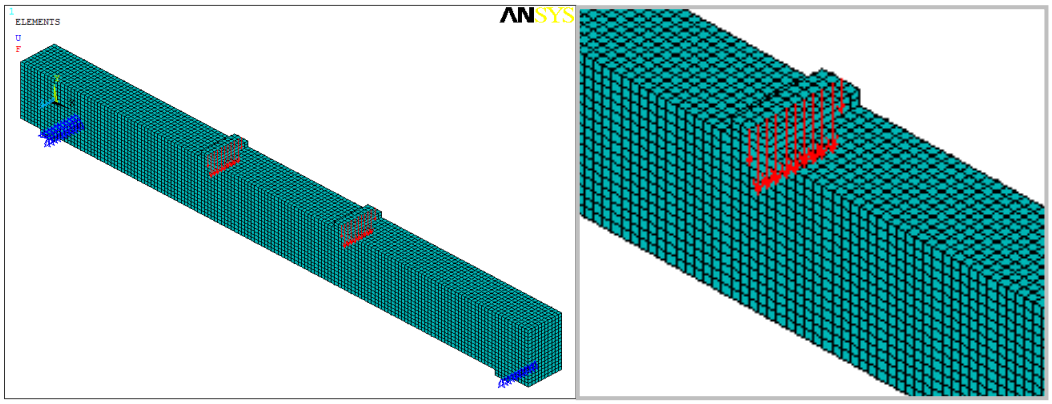

Figure 10: Boundary conditions and external loads for beam **B1**

Presentation of The Ansys Model Results

Results of the modeled beams by **ANSYS** computer program are represented by the load versus midspan deflection relationships and the predicted deformed shapes presentation of the maximum vertical displacement values under effects of the maximum loads. Fig. 11 shows the load versus midspan deflection curves of the modeled beams.

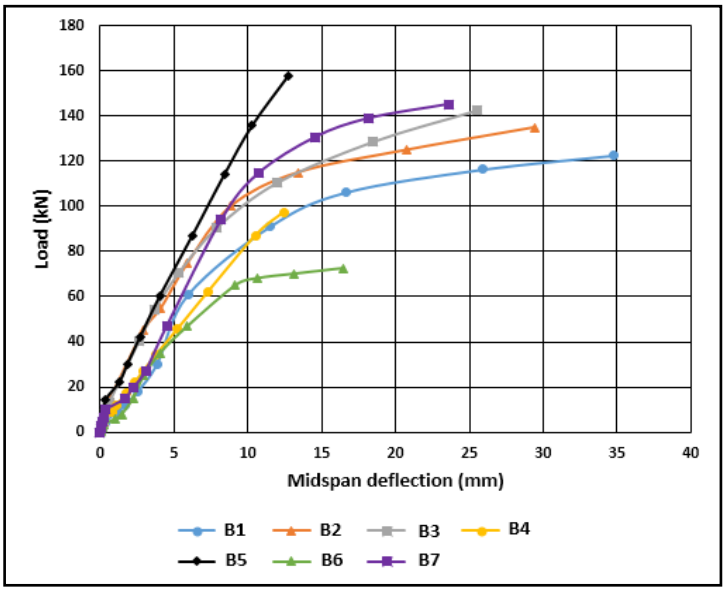

Figure 11: Load versus midspan deflection relationships for the seven tested beams given by the present finite element model of ANSYS program

From observation of Fig. 11 the following behavior is noticed:

a) The addition of steel fibers with volume fraction **0.2%, 0.5%** and **0.8%** to the beams has led to *increases in the ultimate load value* by **4.65%**, **11.92%** and **14.68%**, respectively and percentage decreases in midspan deflection values equal to **12.2%, 23.2%** and **35.5%**, respectively.

b) **100%** *increase* in the *shear-connector spacings* causes *decrease* in the lateral load-

carrying capacity by **26.71%** and the midspan deflection by **52.2%**.

c) *Thickening* of the steel plate by **58.3%** produces percentage *increase* in the ultimate load values equal to **14.37%** and *reduction* in midspan deflection by **57.32%**.

d) However, the ultimate load-carrying capacity suffers *drastic drop* reaching **56.48%** accompanied with a significant *increase* in the midspan deflection reaching **48.39%**, with **40%** *decrease in the steel plate length*.

Figure 12 show the deformed shape of the beam B1 as predicted by the **ANSYS** computer program model.

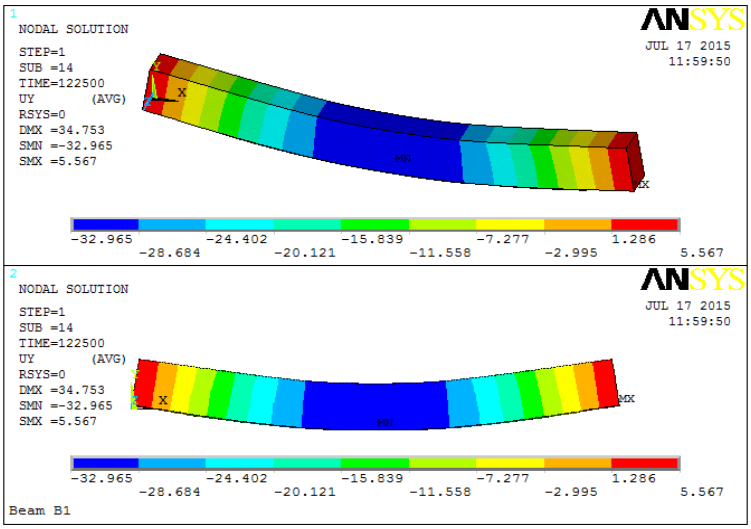

Figure 12: Deformed shape at ultimate stage for beam **B1** predicted by the present ANSYS model

Assessment Of The Numerical Model Theme:

A quantitative evaluation of the accuracy and reliability of the proposed **ANSYS** model is carried out herein. It is represented by a study on the correlation between the numerical model prediction and the experimental evidence. Specifically, a comparative precise inspection of the load versus midspan deflection relationships determined by the **ANSYS** model and those obtained from the present experimental testing of the seven composite reinforced concrete beams fabricated and loaded till failure in the present study has recently been performed. In addition, a close comparative insight into the fracture pattern at failure predicted by the numerical model and its associated ones obtained experimentally is given.

Assessment of the numerical model predictions is set forth in three comparative respects, as follows:

First Respect of Assessment; Comparisons of Load Versus Deflection Relations:

Results of the load versus midspan deflection relationships obtained from the present **ANSYS** model are compared with the experimental load versus midspan deflection ones. Good agreement can be observed in this comparison between **ANSYS** model results and the experimental ones presented in Figs. 13 to 19.

A relatively stiffer numerical curve is obtained at post-cracking stages of behavior.

The numerical ultimate load was slightly higher than the experimental value while the numerical ultimate mid-span deflection was slightly lower.

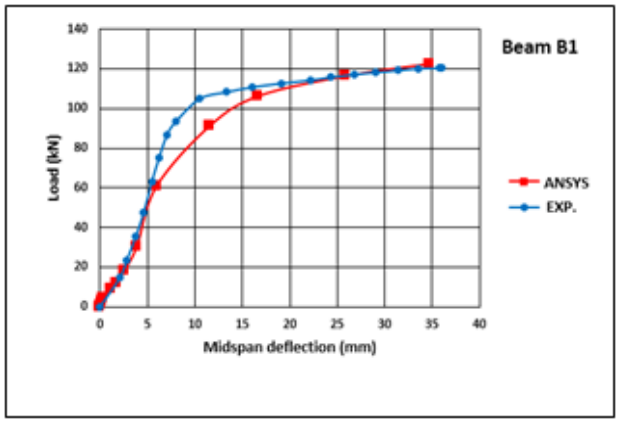

Figure 13: Load versus midspan deflection relationships till failure obtained from the present **ANSYS** model and from experimental for beam **B1**

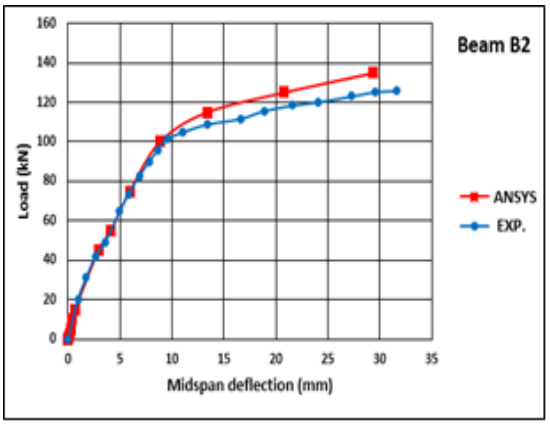

Figure 14: Load versus midspan deflection relationships till failure obtained from the present **ANSYS** model and from experimental for beam **B2**

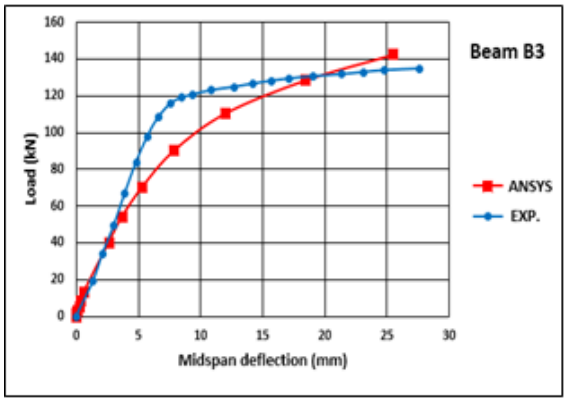

Figure 15 Load versus midspan deflection relationships till failure obtained from the present **ANSYS** model and from experimental for beam **B3**

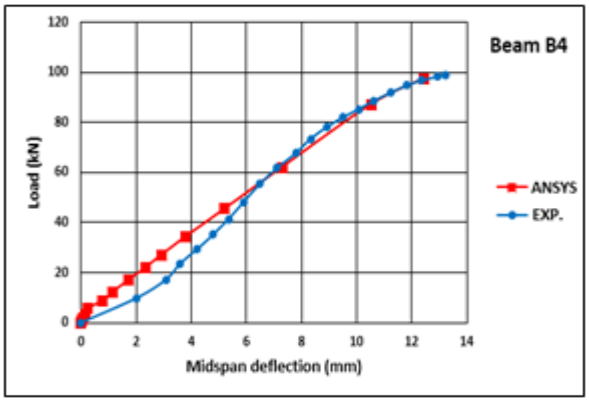

Figure 16: Load versus midspan deflection relationships till failure obtained from the present **ANSYS** model and from experimental for beam **B4**

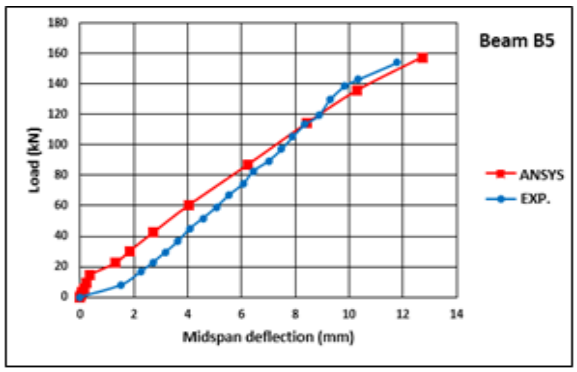

Figure 17: Load versus midspan deflection relationships till failure obtained from the present **ANSYS** model and from experimental for beam **B5**

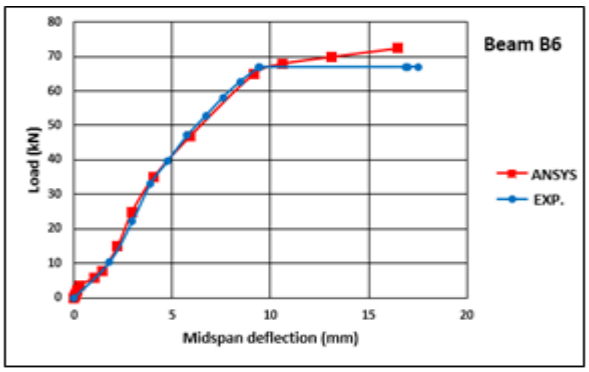

Figure 18: Load versus midspan deflection relationships till failure obtained from the present **ANSYS** model and from experimental for beam **B6**

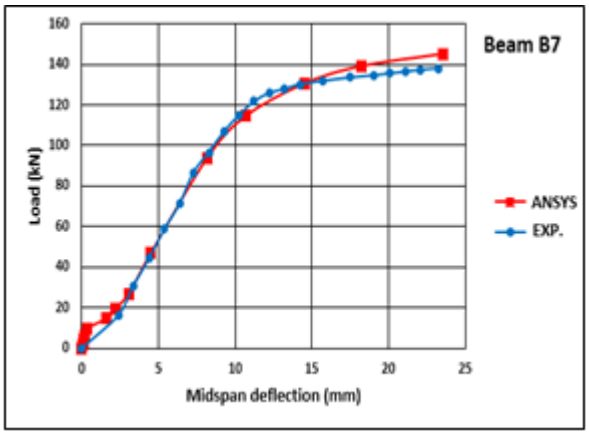

Figure 19: Load versus midspan deflection relationships till failure obtained from the present **ANSYS** model and from experimental for beam **B7**

Second Respect of Assessment; Difference in Ultimate Load and Midspan Deflection Values:

According to Table 8 which presents values of the ultimate loads and the accompanying midspan deflections for the ANSYS model and the experimental investigation for each of the seven "composite reinforced concrete" test beams and their percentages of difference, the main difference percentages between the numerical and experimental ultimate load and their midspans deflections are drawn then presented herein:

i) The *absolute maximum* percentage difference for *the ultimate load values* of the seven test beams is noticed in beam **B6**, where a value of **8.1%** is obtained.

ii) The *average* percentage difference for the ultimate load values of the seven test beams is only **4.5%**.

iii) The *absolute maximum* percentage difference for the *midspan deflection* values at the ultimate stage is **7.8%** for beam **B5**.

iv) However, the corresponding *average* percentage difference of the *ultimate midspan deflection* is *as low as* **5.62%**.

Table 8 : Numerical values of the ultimate loads and the maximum midspan deflections for experimental and ANSYS model results and their difference percentages

Modeled Beams	Ultimate load P_u (KN)			Mid span deflection Δ_u(mm)		
	Experimental	ANSYS	% Diff.	Experimental	ANSYS	% Diff.
B1	120.4	122.5	1.74%	36.02	34.75	3.53%
B2	126	135	7.14%	31.62	29.4	7.02%
B3	134.76	142.5	5.74%	27.65	25.51	7.74%
B4	98.77	97.5	1.29%	13.22	12.44	5.9%
B5	154.12	157.5	2.19%	11.8	12.72	7.8%
B6	67.07	72.5	8.1%	17.51	16.47	5.94%
B7	138.08	145.16	5.13%	23.25	23.58	1.42%
	Mean Ult. Load Difference		4.5%	Mean Deflection Difference		5.62%

Third Part of Assessment; Concrete Fracture Pattern at Failure:

On precise comparative inspection of the concrete fracture patterns at failure of beam **B6**, as resulted from test and predicted by the proposed **ANSYS** model –which are shown in Fig. 20 below, *a perfect coincidence* is observed.

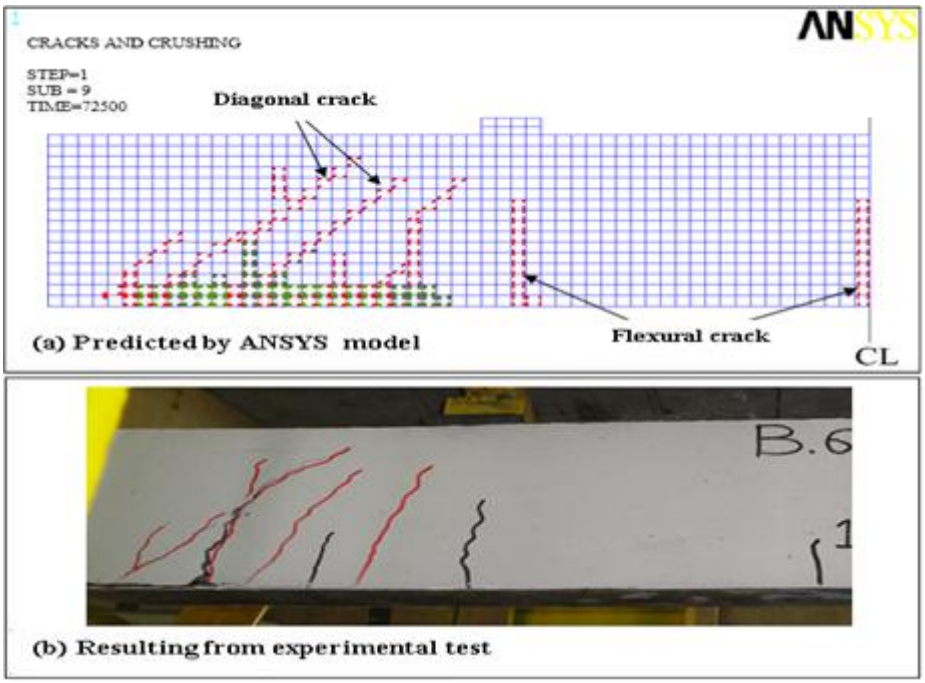

Figure 20 : Concrete fracture patterns at failure for beam B6

Conclusions

The present nonlinear three dimensional finite element model by **ANSYS 14** program has proved to be suitable to predict the flexural behavior of simply supported steel plate-concrete composite (**SPCC**) beams, the program has sufficient accuracy and high level of reliability to be used for structural analysis purposes especially in the ultimate stage to determine the associated loads and deflections. This is demonstrated through comparisons with the experimental evidence in the following sections:

1- Ultimate loads:

The *absolute maximum* percentage of discrepancy between the experimental and the finite element values of the ultimate load for all tested beams is **8.1%,** while the average percentage of discrepancy for the seven tested beams is **4.5%**.

2- Midspan deflections:

The *absolute maximum* percentage of discrepancy between the experimental and the finite element values of the midspan deflection at the ultimate stage for all tested beams is **7.8%,** while the corresponding average percentage difference for the seven tested beams is **5.62%**.

3- Fracture mechanisms:

The present numerical model precisely predicts the unified fracture mechanism for a typical specimen of the *SPCC beams* which consists of the two equally-contributing crack-pattern components: *the flexural crack pattern* at near midspan and the *diagonal-tension crack pattern* within the two exterior thirds of the beam spans

References

[1] Nie Jianguo, Zhu Linsen, and Ren Mingxingl (2001), **"Application of Steel and Concrete Composite Structures in Rehabilitation of Passageways in Beijing, Building Structure"**, Vol. 31, p. 56-57.

[2] Nilson, A. H., Darwin, D., Dolan, C. W., **"Design of Concrete Structures"**, 14th Edition, McGraw-Hill, Inc. 2010.

[3] **"ANSYS Manual"**, Version 14.0, 2009.

[4] Madana, S.K., Kumar, G. R. and Singh, S.P., 2007 **"Steel Fibers as Replacement of Web Reinforcement for RCC Deep Beams In Shear"** Asian Journal of Civil Engineering (Building And Housing) Vol. 8, No. 5, Pages 479-489

[5] Lihua, X., Yin, C., Jie, S., and Dongtao, X., 2008, **"Nonlinear Finite Element Analysis of Steel Fiber Reinforced Concrete Deep Beams"**, Wuhan University, Journal of Natural Science, Vol.13 No.2, 201-206

[6] Kachlakev, D., Miller, T. and Yim, S., **"Finite Element Modelling of Reinforced Concrete Structures Strengthened with FRP Laminates"**, Final Report, SPR 316, May 2001.

[7] ASTM C1240-03, **"Standard Specification for Use of Silica Fume as a Mineral Admixtures in Hydraulic-Cement Concrete, Mortar, and Grout "**, Annual Book of ASTM Standard, Vol. 15-02, 2005, p. 1-6.

[8] Wolanski, A. J., **"Flexural Behaviour of Reinforced and Prestressed Concrete Beam using Finite Element Analysis"**, M.Sc. Thesis, Marquette University, May 2004.

[9] Amer M. Ibrahim, Mohammed Sh. Mahmood (2009) **"Finite Element Modeling of Reinforced Concrete Beams Strengthened**

with FRP Laminates", Paper, College of engineering , Diyala University, Iraq.

[10] Agwan, A. A., August 1996**, "Nonlinear Finite Element Analysis of Steel Fiber Reinforced Concrete Members"**, Mosul University, Iraq, pp. 237.

[11] Al-Taee, M. J., **"Experimental and Finite Element Investigation of Longitudinal Shear Resistance for Composite Reinforced Concrete T-Beams Cast in Steel Channel"** M.Sc. Thesis, Department of Civil Engineering, Al-Anbar University, March 2012.

[12] European Committee for Standardisation (CEB), Eurocode 4, **"Design of Composite Steel and Concrete Structures"**, Part 1.1: General Rules and Rules for Buildings, DD ENV 1994-1-1, EC4.

ACI Committee 318, **"Building Code Requirements for Structural Concrete (ACI 318M-08) and Commentary (ACI 318RM-08)"**, American Concrete Institute, Farmington Hills, 2008

.

النمذجة بالعناصر المحددة والتحليل النظري لجسور مركبة من الخرسانة ذاتية الرص المسلحة بألياف حديدية والمقواة بصفائح حديدية سفلية مشدودة

ليث خالد الحديثي
هنــدسة أنشــائية
جامعة النهرين / قسم الهندسة المدنية
E-mail:lthadithy@yahoo.com

مريم عبدالجبار حسن
هندسة أنشائية
جامعة النهرين / قسم الهندسة المدنية
E-mail:maryem_aj@yahoo.com

الخلاصـــة:

البحث الحالي هو دراسة عن النمذجة بالعناصر المحددة والتحليل النظري لتقييم تأثير الالياف الحديدية على تصرف العتبات المركبة ذوات أسطح الحديد – الخرسانة البينية المشدودة المزودة بروابط قص. إعتمادا" على فحوصات عملية لسبع جسور مركبة مكّونة من مقطع خرساني مسلح مستطيل الشكل (125*200*1900)ملم مقوىّ من الاسفل بصفائح حديدية مربوطة بروابط قص, مع أضافة نسب حجمية مختلفة من الالياف الحديدية (0.0%, 0.2%, 0.5% و 0.8%), تغيير توزيع الروابط القصية وسمك الصفيحة وطولها. كل عتبة تم تحميلها تحت تأثير حملين مركزين وتم رصد نمط الفشل وتسجيل قيم الحمل والانحراف عند منتصف العتبة حتى الفشل وايضا" تسجيل قيم الحمل والانزلاق النسبي النهائي لأطراف العتبة. تم التحليل الرقمي لتلك العتبات المركبة السبع باستخدام برنامج ANSYS14 متضمنا تمثيل الخرسانة، حديد التسليح، حديد الصفائح السفلية ومنطقة التماس بين الصفيحة الحديدية والخرسانة. وقد كان التوافق العالي بين تنبؤات النموذج ANSYS والنتائج التجريبية شاهدا" واضحا" على موثوقية النموذج الرقمي, حيث ان اكبر فرق للحمل الاقصى والانحراف الوسطي لجميع الجسور لم يتجاوز 8.1% و 7.8% على التوالي.